

Phillips, C. and Brown, R.E. (2008) Eulerian simulation of the fluid dynamics of helicopter brownout. In: 64th American Helicopter Society Annual Forum, 28 April - 1 May 2008, Montral, Canada.

<http://strathprints.strath.ac.uk/27501/>

Strathprints is designed to allow users to access the research output of the University of Strathclyde. Copyright © and Moral Rights for the papers on this site are retained by the individual authors and/or other copyright owners. You may not engage in further distribution of the material for any profitmaking activities or any commercial gain. You may freely distribute both the url (<http://strathprints.strath.ac.uk>) and the content of this paper for research or study, educational, or not-for-profit purposes without prior permission or charge. You may freely distribute the url (<http://strathprints.strath.ac.uk>) of the Strathprints website.

Any correspondence concerning this service should be sent to The Strathprints Administrator: eprints@cis.strath.ac.uk

Eulerian Simulation of the Fluid Dynamics of Helicopter Brownout

Catriona Phillips *
c.phillips@aero.gla.ac.uk

Richard E. Brown
rbrown@aero.gla.ac.uk

Department of Aerospace Engineering, University of Glasgow
Glasgow G12 8QQ, United Kingdom

Abstract

A computational model is presented that can be used to simulate the development of the dust cloud that can be entrained into the air when a helicopter is operated close to the ground in desert or dusty conditions. The physics of this problem, and the associated pathological condition known as ‘brownout’ where the pilot loses situational awareness as a result of his vision being occluded by dust suspended in the flow around the helicopter, is acknowledged to be very complex. The approach advocated here involves an approximation to the full dynamics of the coupled particulate-air system. Away from the ground, the model assumes that the suspended particles remain in near equilibrium under the action of aerodynamic forces. Close to the ground, this model is replaced by an algebraic sublayer model for the saltation and entrainment process. The origin of the model in the statistical mechanics of a distribution of particles governed by aerodynamic forces allows the validity of the method to be evaluated in context by comparing the physical properties of the suspended particulates to the local properties of the flow field surrounding the helicopter. The model applies in the Eulerian frame of reference of most conventional Computational Fluid Dynamics codes and has been coupled with Brown’s Vorticity Transport Model. Verification of the predictions of the coupled model against experimental data for particulate entrainment and transport in the flow around a model rotor are encouraging. An application of the coupled model to analyzing the differences in the geometry and extent of the dust clouds that are produced by single main rotor and tandem-rotor configurations as they decelerate to land has shown that the location of the ground vortex and the size of any regions of recirculatory flow, should they exist, play a primary role in governing the extent of the dust cloud that is created by the helicopter.

Nomenclature

| | |
|-------------|--------------------------------------|
| d | particle diameter |
| F | drag force on particle |
| g | acceleration due to gravity |
| m | particle mass |
| S_ω | = source of vorticity |
| S_p | source of particulates |
| t | time |
| u | velocity of particle relative to air |
| μ | advance ratio |
| μ^* | thrust normalized advance ratio |
| ν | fluid viscosity |
| ν_p | particle diffusion constant |
| ρ | air density |
| ρ_p | local density of particulates in air |
| ρ_s | material density of particles |
| ς | ‘species’ of particle |

| | |
|------------|---------------------------------|
| v | local flow velocity |
| v_t | threshold velocity |
| v_b | local on-blade velocity |
| v_g | fallout velocity due to gravity |
| v_p | particle velocity |
| ω | vorticity |
| ω_b | blade bound vorticity |

Introduction

A particular concern to helicopter operators in desert or dusty conditions is the possibility of entrainment of dust from the ground into the air when the vehicle is operated close to the ground. This entrainment can cause large clouds of dust to form in the air surrounding the helicopter, and the possibility exists under certain operational conditions that these clouds might obscure the pilot’s view, particularly while landing or taking off. A considerable body of anecdotal evidence from pilots describes how, under the severest conditions, the envelopment of the helicopter in clouds of dust can result in a potentially dangerous con-

*Presented at the American Helicopter Society 64th Annual Forum, Montréal, Canada, April 29 - May 1, 2008. Copyright ©2008 by the American Helicopter Society International, Inc. All rights reserved.

dition known as ‘brownout’ where the pilot loses situational awareness. Although it is unlikely that any remedy for the operational effects of brownout will be entirely aerodynamic in origin, there is the strong possibility that an improved understanding of the fluid dynamics of brownout may lead to measures that might ameliorate its effects. Indeed, some recent reports have claimed that the specifics of rotor geometry may have significant impact on the spatial extent and rate of formation of the dust cloud as brownout conditions develop in the airflow surrounding the helicopter.

Perhaps not surprisingly, given the recency of the events that have promoted a resurgence of interest in the brownout phenomenon, very little work has been published to date that investigates in any detail the governing physics behind its onset. Although a fairly large number of works exist that detail both observational and theoretical studies of the transport of particulate matter by air or water, this literature has originated primarily from within the field of riverine and aeolian sedimentology. A large body of information and a number of empirical models do exist for the behavior of particulate matter suspended in water and air, but these models have generally been derived for flows found in nature where the fluid length- and time-scales are somewhat different to those associated with flow conditions in the helicopter wake. In the helicopter context, very limited experimental data exists and, although some significant progress has been made, it is fair to say that modeling of brownout and its development is still in its infancy. Indeed, in the helicopter context, much remains to be understood at a very fundamental level.

Currently most approaches to the modeling of brownout have been formulated in the particle-fixed Lagrangian frame of reference. In this approach, the dynamics of a (very large) number of individual dust particles is tracked as they are carried along in the air-flow that is generated by the helicopter. The properties of the resultant dust cloud are then inferred from the behavior of this representative set of particles. Previous work in this vein includes that of Keller et al. (Ref. 1) and Leishman’s group at the University of Maryland. Good qualitative results are possible using the Lagrangian approach, but the detailed dynamics of a very large number of particles need to be modeled if an accurate measure of the prime variable influencing brownout, i.e. the distribution of dust density within the flow around the helicopter, is to be obtained. The computational requirements of the Lagrangian approach can become very large and the formal accuracy of its predictions can be difficult to quantify rigorously. CFD-type methods for the rotor flow itself are generally formulated in the Eulerian, i.e. helicopter- or ground-fixed frame of reference. A very much more convenient representation of the brownout problem would thus result from modeling the dynamics of the particulate distribution in the air surrounding the helicopter using an Eulerian approach where the evolution

of the dust density distribution is calculated directly using suitable transport equations.

Given the importance of aerodynamic forces in governing the trajectory of the particles through the air, a formalism that relies on a coupled system of mass and momentum transport equations to encapsulate the behavior of the fluid, and any particulate matter suspended within it, would seem to yield the most logical and physically complete approach to modeling the dynamics of brownout. The ‘multi-phase’ formalism that is required to implement this approach is relatively well developed within the chemical processing industry, for instance (see Ref. 2). In applying this approach in its full rigor to the brownout problem there is the distinct possibility though that the parameters that are required to characterize the interactions between the various particulates, and the particulates and the air, may in fact be unknown or only amenable to crude estimation – especially given the diversity of particle sizes and types that are involved. Arguably, a model that contains too many free parameters is of little use from an engineering perspective in any case because of the lack of robustness of its predictions to variation in its parameters (the Occam’s Hill scenario described by Leishman in Ref. 3). There is thus considerable merit, particularly at our present level of understanding of the brownout phenomenon, in developing a robust model with as few free parameters as possible in order to reduce the sensitivity of predictions to errors in capturing the fine details of the behavior of the particulates during the formation of the brownout cloud.

In this vein, Ryerson et al. (Ref. 4) have produced a model for the dynamics of the dust cloud that uses a two-phase mass transport equation to represent the suspended particulate matter as one of two co-existing but continuous fluid phases within the flow around the helicopter. The suspended particulate matter is assumed to be convected at the local velocity of the air, offset by a fallout velocity to account for the effects of gravity. Such an approach has the advantage of forgoing any explicit accounting for the momentum interchange between the fluid and the suspended particulate matter, and hence any requirement for explicit characterization of the interactions within the system, but must thus necessarily involve some approximation to the dynamics of the suspended particulate matter. The limits to the applicability of the simplified mass-transport approach in the context of brownout modeling has yet to be rigorously explored, however.

In this paper, an approximate form for the continuum equations of motion describing the transport of particulates in the Eulerian reference frame is derived from the basic principles of statistical mechanics, beginning from the Newtonian dynamics of individual particles. This approach neatly reconciles the Lagrangian and Eulerian descriptions of the particulate transport problem and yields a mass transport equation that can be used to analyze the physics of brownout from within the Eulerian frame of ref-

erence. The model that results from the analysis is similar in structure to the mass transport equations of Ryerson et al. (Ref. 4), but the foundation of the model in the aerodynamic behavior of the individual particles that constitute the cloud of suspended matter allows the validity of the approach to be estimated directly in terms of the properties of the flow in the wake of the helicopter.

An extension of Brown's Vorticity Transport Model (VTM) (Refs. 5, 6) that includes this model for the entrainment and transport of particulates is then described in some detail. One of the main benefits of using the VTM to support the particulate transport model is that a particularly efficient computational formulation of the brownout problem can be obtained due to the similarities between the Eulerian formulation of the particle transport equation and the vorticity transport equation.

Given the extraordinary complexity of the physics in the ground layer, it proves impossible – given the current state of knowledge – not to introduce a fairly large element of semi-empiricism into any self-contained model that is capable of predicting the dynamics of particulate flows that are driven by the interaction of the helicopter wake with the ground. Various insights into the dynamics of particulate motion along the ground and the entrainment of particles into the air-flow are borrowed from the environmental fluid dynamics community to construct the various semi-empirical constituents of the brownout model that is described in this paper. Further analysis and verification will reveal if the particular selection of empirical models described here is the most appropriate for the modeling of the onset and development of brownout conditions surrounding the helicopter. Notwithstanding, the resultant model is used to simulate the evolution of the dust cloud that is generated by two coupled rotor-fuselage configurations in strong ground effect – one representing a conventional helicopter with a single main rotor and the other a tandem configuration – when operated at low altitude above a dusty surface. These initial computations illustrate the capabilities of the model and, indeed, reveal some significant differences between the dust cloud that is generated by these two configurations. These differences are, to a large degree, consistent with anecdotal evidence.

Vorticity Transport Model

A model for the transport of particulates in the air flow surrounding the helicopter has been integrated into Brown's Vorticity Transport Model (Refs. 5, 6). The VTM is a finite-volume method that calculates the evolution of the vorticity distribution on a structured computational mesh surrounding the rotorcraft by evolving the solution to the vorticity-velocity form of the incompressible Navier-Stokes equation,

$$\frac{\partial}{\partial t}\omega + v \cdot \nabla\omega - \omega \cdot \nabla v = S_\omega + \nu\nabla^2\omega \quad (1)$$

through time. The velocity with which the vorticity is convected through the flow is related to the vorticity by the differential form of the Biot-Savart relationship,

$$\nabla^2 v = -\nabla \times \omega \quad (2)$$

The vorticity source, S_ω , arises in the shed and trailed vorticity from the lifting surfaces immersed within the flow, and can be written as

$$S_\omega = -\frac{d}{dt}\omega_b + v_b \nabla \cdot \omega_b \quad (3)$$

where ω_b is the bound vorticity associated with each surface.

Particle Transport Model

In the Lagrangian frame of reference, the dynamics of a single particle (with mass m) is given by Newton's second law

$$m \frac{dv_p}{dt} = F \quad (4)$$

where F is the force applied to the particle. If gravity and aerodynamic drag are assumed to be the dominant forces acting on the particle, then Rayleigh's expression

$$F(u) = -\frac{1}{2}\rho|u|u\frac{\pi d^2}{4}C_D + mg \quad (5)$$

is often used to describe the force applied to a particle with diameter d , where $u = v_p - v$ is the particle velocity v_p relative to the air velocity v . The drag coefficient C_D of the particle is generally also a function of u (i.e. of the particle Reynolds number Re) and for very small particles $C_D = 24/Re$ yields a result that is consistent with Stokes's well-known expression

$$F(u) = -3\pi\rho\nu ud + mg \quad (6)$$

for a sphere moving through a viscous fluid.

To derive the equation that governs the transport of a large number of suspended particles in the ground or helicopter-fixed Eulerian frame of reference, the most robust approach results from adopting the formalism of classical statistical mechanics. Let the spectrum of particles present in the flow be defined by some (continuous) variable ς representing the 'species' of any particle as distinguished by its mass, size or other relevant physical characteristics. Define the particle probability density function $\Phi(x, v, \varsigma, t)$ so that $\Phi(x, v, \varsigma, t)\Delta x\Delta v\Delta\varsigma$ is the probability of finding a particle of species within the range $\Delta\varsigma$ containing ς , traveling with velocity within the range Δv containing v , within the region of space Δx surrounding x at time t . Assume that the particles are sufficiently dilute once they are suspended within the air for collisions to be rare (so that the forces associated with collision do not need to be

accounted for) and so that the reaction of the particles on the air can be neglected. Assume also that the particles do not break up or coalesce (so that the species distribution of the particles does not change with time). Newton's second law can then be expressed in terms of the evolution of the particle probability density function as

$$\Phi(x + v\Delta t, v + F\Delta t/m, \varsigma, t + \Delta t) = \Phi(x, v, \varsigma, t) \quad (7)$$

where $F(x, v, m)$ is the force experienced by a particle with mass $m(\varsigma)$ and velocity v traveling through the point x (and hence is given by Eq. 4). In the infinitesimal limit $\Delta t \rightarrow dt$, this expression reduces to the Liouville equation

$$(\partial/\partial t + v \cdot \nabla + F/m \cdot \nabla_v) \Phi(x, v, \varsigma, t) = 0 \quad (8)$$

For the purposes of predicting brownout, the assumption is then made that the evolution of the particle distribution is governed by two physical processes that have highly disparate timescales. Specifically, it is assumed that the convective motion of the particles as they are carried along with the air flow is slow compared to the acceleration of the particles in response to any imbalance in the forces acting upon them, or, in other words, if $\dot{u} \neq 0$, $\dot{u} \gg \dot{v}$ no matter what the acceleration of the flow \dot{v} . Given the structure of Eq. 5 or Eq. 6 this assumption implies that the particles will remain in near-equilibrium under the action of the aerodynamic forces that are generated by the particle as they move relative to the air (i.e. the dynamics of any individual particle is such that the net force F acting on any particle remains small). This near-equilibrium assumption is justified below in the context of the typical particle sizes involved in creating the dust cloud that is responsible for brownout.

From either Eq. 5 or Eq. 6, exact equilibrium in the Lagrangian sense implies that $v_p = v - v_g$, where v_g is the 'fallout velocity' of the particle due to gravity. In the Eulerian frame of reference, the assumption of near-equilibrium allows Eq. 8 to be factored into a 'fast' equation

$$(\partial/\partial t + F/m \cdot \nabla_v) \Phi(x, v, \varsigma, t) = 0 \quad (9)$$

and a 'slow' equation

$$(\partial/\partial t + v \cdot \nabla) \Phi(x, v, \varsigma, t) = 0 \quad (10)$$

The solution to the fast equation can easily be shown to be a particle probability density function that concentrates ever more closely on the equilibrium Lagrangian particle velocity $v_p = v - v_g$ as time proceeds¹.

The number density of particles at point x in the flow with species within the band $\Sigma = [\varsigma^-, \dots, \varsigma, \dots, \varsigma^+]$ can be obtained from the particle probability distribution func-

tion as

$$\begin{aligned} \rho_p(x, \Sigma, t) &= \int_{-\infty}^{\infty} \int_{\varsigma^-}^{\varsigma^+} \Phi(x, v, \varsigma, t) d\varsigma dv \\ &\equiv \int_{\Sigma, v} \Phi(x, v, \varsigma, t) d\varsigma dv \end{aligned} \quad (11)$$

Applying this operator to the slow component, Eq. 10, of the Liouville equation gives

$$\int_{\Sigma, v} (\partial/\partial t + v \cdot \nabla) \Phi d\varsigma dv = 0 \quad (12)$$

which can be expanded as

$$\frac{\partial}{\partial t} \int_{\Sigma, v} \Phi d\varsigma dv + \int_{\Sigma, v} (v \cdot \nabla \Phi) d\varsigma dv = 0 \quad (13)$$

From Eq. 11 the first term in this expression is simply $\partial\rho_p/\partial t$. By the Midpoint Theorem the second term can be written as

$$\bar{v} \cdot \nabla \int_{\Sigma, v} \Phi d\varsigma dv + \int_{\Sigma, v} (v' \cdot \nabla \Phi) d\varsigma dv \quad (14)$$

where the species-dependent ensemble velocity

$$\bar{v}(\Sigma) = \frac{\int_{\Sigma, v} \Phi v d\varsigma dv}{\int_{\Sigma, v} \Phi d\varsigma dv} \quad (15)$$

Given the structure of the solution to the fast component of the Liouville equation, for a system of particles close to equilibrium, the Lagrangian equilibrium velocity v_p for particles with species ς is a very good approximation to $\bar{v}(\Sigma)$. This allows the first term of Eq. 14 to be interpreted as representing the convection of the particle distribution by the air flow under conditions of force equilibrium. The second, 'residual' term then represents the transport of particles due to non-equilibrium of the system (i.e. due to scatter of the particle velocities about their equilibrium values). This second term can be modeled in various ways. For instance, if a symmetric distribution of velocities about equilibrium is assumed, then this term can be represented as an isotropic diffusion term $\nu_p \nabla^2 \rho_p$ (but where the diffusion coefficient is species-dependent, ie $\nu_p = \nu_p(\Sigma)$). Alternatively, a more sophisticated non-isotropic model can be adopted to capture the skew of the particle velocity distribution about equilibrium, for instance by including a dependence on vorticity gradients in the flow to model the centrifugal spin-out of particles from vortex cores.

Thus the transport equation for the particulates within the species band Σ can be written as

$$\begin{aligned} \frac{\partial}{\partial t} \rho_p + (v + v_g) \cdot \nabla \rho_p &= S_p + \nu_p \nabla^2 \rho_p \\ &+ \text{other non-equilibrium terms} \end{aligned} \quad (16)$$

¹That is, as $t \rightarrow \infty$, $\Phi(x, v, \varsigma, t) \rightarrow 0$ for all $v \neq v_p$.

where the source term $S_p(\Sigma)$ is introduced to allow the addition of particulates into the flow by entrainment from the ground. The assumption of the absence of collisions between particles allows any significant variations in the physical properties of the particulate matter within the flow to be accommodated by grouping the particulates into a number of species bands $\Sigma_1, \dots, \Sigma_N$ and solving an independent transport equation for each band.

Particle Equilibrium

For the equations derived above to yield an adequate description of particulate transport under brownout conditions, it remains to justify the principal underlying assumption of the analysis that the airborne particulates that are responsible for brownout conditions exist in a state of near-equilibrium with the aerodynamic and gravitational forces that act upon them. Newton's equation, Eq. 4, can be recast in terms of the relative velocity between fluid and particle as

$$\dot{u} + F(u)/m = \dot{v} \quad (17)$$

Consider the special case in the absence of gravity, so that particle force equilibrium is attained when $u = 0$. If the condition $\dot{u} \gg \dot{v}$ for near-equilibrium of the particles does apply when $\dot{u} \neq 0$, then, for instance given Stokes's drag law (similar results can be derived for other drag models),

$$u \approx \dot{v}/\Gamma \quad (18)$$

is an approximate solution to Eq. 17, where the particle 'drag to mass ratio' (the reciprocal of the 'particle velocity response time' used commonly in the multi-phase fluid dynamics literature)

$$\Gamma = 18 \frac{\rho}{\rho_s} \frac{\nu}{d^2} \quad (19)$$

The relative local deviation of the particle dynamics from equilibrium is thus small if u is small relative to v , in other words if $\Gamma \gg |\dot{v}|/|v|$, that is, if the drag to mass ratio of the particles is large compared to the local acceleration of the flow (scaled by the local velocity of the flow) in the Lagrangian, or particle, frame of reference.

Figure 1 shows typical values for the particle drag-to-mass ratio Γ (assuming the particle drag to be given by Stokes's law – note that this model under-estimates the aerodynamic drag of large particles) as a function of the particle size parameter $\rho_s d^2$ for the variety of different particle types that might constitute the ground surface below the helicopter.

For comparison, Fig. 2 shows a typical distribution of the Lagrangian acceleration parameter $|\dot{v}|/|v|$ within the flow in the wake below an isolated helicopter rotor operating in strong ground effect, as predicted using the VTMs. In this example the rotor is flying 0.68 radii above the ground at an advance ratio of 0.05. The data is scaled

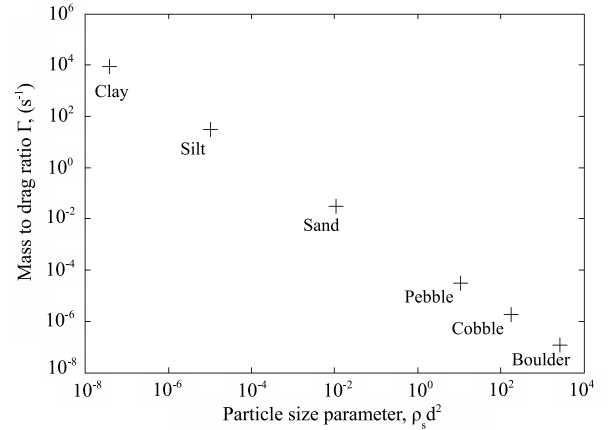
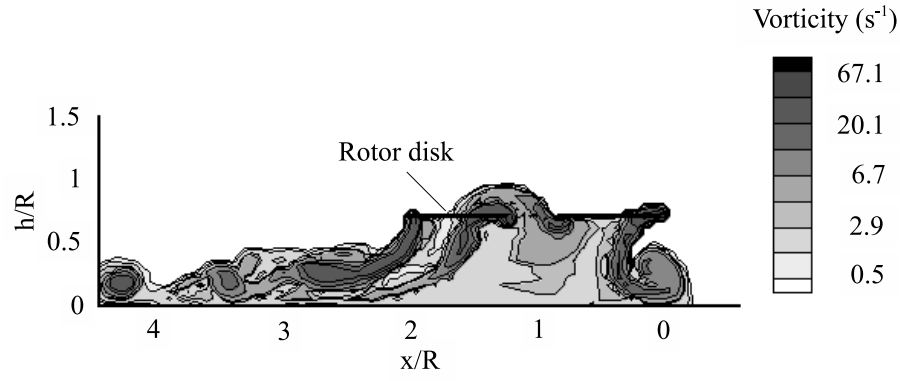


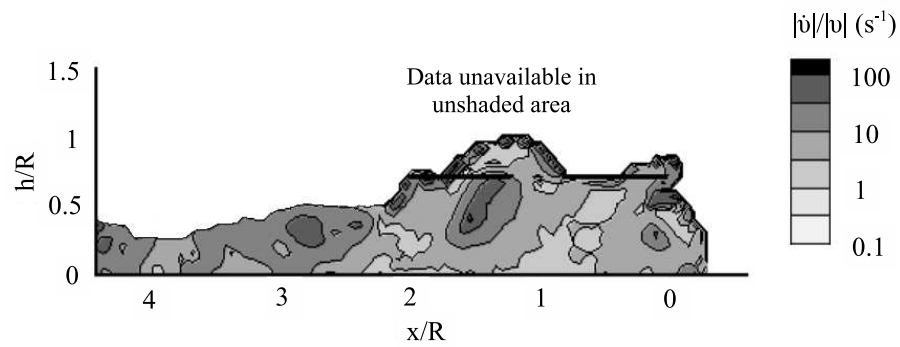
Figure 1: Particle drag to mass ratios for various sizes of particle commonly encountered in the desert environment.

to be representative of a helicopter in the same class as a UH-60 Blackhawk. The Lagrangian acceleration parameter is calculated from the Eulerian velocity distribution in the flow surrounding the helicopter according to the equivalence $\dot{v} = \partial v / \partial t + v \cdot \nabla v$. It is important to bear in mind when analyzing this figure that the finite resolution of the computation results in any local maxima in the Lagrangian acceleration parameter being under-estimated, as any non-resolved finer structures in the flow will contribute significantly to the local acceleration through the term $v \cdot \nabla v$.

Comparing Figs. 1 and 2 shows that the question of the validity of the Eulerian transport equations derived earlier as a model for particulate transport in the helicopter flow field needs to be approached with some care. For given local flow conditions, the assumption of near-equilibrium becomes increasingly valid the smaller and lighter the particulate matter. The analysis of particulate transport using the Eulerian approach presented above, even when corrected for non-equilibrium effects by the addition of suitable terms to the transport equation, would be somewhat tenuous throughout the rotor flow field when the behavior of large objects such as pebbles, rocks and other debris is important – such as in the analysis of helicopter-induced damage and erosion for instance. In these cases, the traditional approach through calculation of the Lagrangian dynamics of individual particles within the flow is likely to remain the most reliable and efficient. Similarly the analysis for particles with intermediate size (e.g. sand) is likely to prove satisfactory only if augmented by terms, as described above, representing the non-equilibrium behavior of the particles. Much anecdotal evidence suggests though that the principal composition of the brownout cloud is extremely fine, powder-like particulate matter, and for this application the comparison presented here suggests that for realistic helicopter weights and sizes the near-equilibrium assumption, and hence the analysis of the brownout prob-



(a)



(b)

Figure 2: Snap-shots of the instantaneous flow properties on a vertical slice through the centerline of an isolated rotor flying at $0.68R$ above the ground at an advance ratio of 0.05 ($C_T = 0.0048$). (a) Contour plot of vorticity magnitude, showing the rotor to be in the ground vortex regime. (b) Plot showing the resultant distribution of the Lagrangian acceleration parameter $|\dot{v}|/|v|$ in the rotor wake (data scaled for a Blackhawk-sized aircraft).

lem using the particulate transport equations derived above, remains well-founded throughout most of the flow surrounding the helicopter – with perhaps the exception being near the cores of the individual vortices that constitute the rotor wake, and very close to the rotor itself.

Particle Entrainment Model

The source term S_p in the particle transport equation accounts for the entrainment of particulates from the ground into the airflow. In the context of brownout modeling, the model for the source term provides essentially a ‘sublayer’-type description that captures the essence of the complex physics that takes place within the few inches of fluid just above the ground. In much the same fashion as a boundary layer model matches the viscous, possibly turbulent characteristics of the flow near the surface to a simplified model that approximates the fluid behavior away from the surface,

the model for the particulate source S_p is used to represent the effect of the physics in the sublayer on the dynamics of the particulate distribution in the flow away from the surface. In particular, within the sublayer the particulate density can be high and the collisions between particles may assume fundamental importance – in direct variance with the assumptions made earlier in deriving the particulate transport equations.

According to Marticorena and Bergametti (Ref. 7) entrainment of dust into the air takes place only if the velocity of the air just above the ground surface exceeds the minimum, or threshold, velocity required to initiate particle motion along the surface. The larger particles then hop along the surface in a motion called ‘saltation’, and the impact of these saltating particles with the surface causes further particles to be ejected from the surface. Instead of returning to the surface, though, the smallest ejected particles are entrained into the flow above the ground.

The physics of particle entrainment into the flow is thus very complex. Direct modeling of the dynamics of saltating particles is well beyond the present state of the art, but there exists a number of empirical models for the saltation process that are able to take into account various factors such as surface roughness, soil moisture and soil crusting. Models of this complexity may be useful in capturing the detailed behavior of the ground surface in specific geographical areas, but in the present work a simpler semi-empirical model,

$$v_t = \frac{1}{\kappa} \sqrt{a_1 \left(\frac{\rho_s}{\rho} g d + \frac{a_2}{\rho d} \right)} \quad (20)$$

that represents the threshold velocity for flow over dry, loose soil surfaces is used. On the basis of wind tunnel measurements by Lu and Shao (Ref. 8), the coefficients a_1 and a_2 are approximately 0.0123 and $3 \times 10^{-4} \text{ kgs}^{-2}$ respectively. The factor κ accounts for the presence of surface roughness elements. Many different roughness elements can be present in an actual desert environment but to simplify the model only one type is considered in the calculations presented in this paper. It is assumed simply that there are fragments of rock present that armor the surface and inhibit the entrainment of particulates into the flow. According to MacKinnon (Ref. 9), the value of κ for this type of surface is 0.44. For simplicity, the results presented in this paper were generated after adopting a single representative value of saltating particle diameter d and density ρ_s , and hence a uniform threshold velocity over the entire ground surface is assumed.

The overall source of particulate matter into the flow is dependent on the flux of saltating particles along the ground. The saltation or horizontal particle flux, Q , is determined using the theory of White (Ref. 10) where the horizontal particle flux is related to the flow velocity v just above the surface by

$$Q = E c v^3 \frac{\rho}{g} \left(1 - \frac{v_t}{v} \right) \left(1 + \frac{v_t^2}{v^2} \right) \quad (21)$$

where v_t is the threshold velocity calculated from Eq. 20. Empirically, $c = 0.261$, and E is the ratio of erodible to total surface area, taken for simplicity to be unity in the calculations presented in this paper.

The particle flux from the surface into the airflow above the surface then consists of those dust particles that are released from the saltation process and remain in suspension in the air above the ground. The ratio of the particle flux into the air to the saltation flux is dependent on the percentage of clay within the soil. In the current model, the empirical relationship

$$S_p = Q e^{13.4f-6.0} \quad (22)$$

described in Ref. 7 is used to relate the source S_p of particulate matter into the flow to the saltation flux. This re-

lationship applies for soils with clay fraction f less than 0.2; all results presented in this paper were generated using $f = 0.1$.

Particle Fallout Model

The fallout velocity v_g in Eq. 16 accounts for the tendency of suspended particulate matter to settle out from the flow under the influence of gravity. The model that was used to calculate the fallout velocity for the calculations presented in this paper is based on the work by Cheng (Ref. 11) which extends Stokes's solution for the settling velocity of spherical particles to allow it to be used when the particle Reynolds number is greater than one. The dimensionless particle diameter, d_* , is first defined as

$$d_* = d \left(\frac{g b}{\nu^2} \right)^{(1/3)} \quad (23)$$

where $b = (\rho_s - \rho)\rho$. The fallout velocity of the particles is then given by

$$v_g = \frac{\nu}{d} \left(\sqrt{25 + 1.2 d_*^2} - 5 \right)^{1.5} \quad (24)$$

Computational Implementation

There are obvious similarities between the mathematical form of the vorticity transport equation, Eq. 1, and the particulate transport equation, Eq. 16. Both equations (when taken at face value) represent the passive advection of some quantity by a background velocity field, and allow for a localized source of the advected quantity. In the case of the vorticity transport equation an additional stretching term appears simply to account for the fact that the advected quantity (the vorticity) is fundamentally vectorial in nature rather than scalar as in the case of the particulate density. The similarity in structure between the two transport equations allows the procedure that is used within the VTM to calculate the evolution of the vorticity within the flow simply to be generalized slightly if the combined evolution of the flow and particulate density is to be calculated. For the combined particulate-vorticity transport model, define the vector of conserved variables $\Omega(x, t) = (\omega, \rho_p^1, \dots, \rho_p^N)$ where $\rho_p^i(x, t)$ is the local density of particles in species band Σ_i at time t . The object-oriented structure of the VTM allows the augmented vector Ω of conserved variables simply to be defined as a generalized form of the vector of conserved quantities ω that is used by the original, fluid-only version of the code. The VTM uses an operator-splitting approach to evolve the equations of motion for the coupled system. The source of Ω into the computational domain is first calculated by evolving the equation

$$\frac{\partial}{\partial t} \Omega = S \quad (25)$$

over time Δt , using the initial condition $\Omega(x, t)$ to yield the intermediate solution $\Omega^*(x)$. The combined particulate / vorticity source $S = (S_\omega, S_p^1, \dots, S_p^N)$ is constructed using the appropriate physical model for each component. The advection equation

$$\frac{\partial}{\partial t} \Omega + V \cdot \nabla \Omega = 0 \quad (26)$$

is then advanced through Δt , using Ω^* as initial condition, to yield the revised intermediate solution Ω^{**} . The advection velocity $V = (v, v + v_g)$, and the operator $a \cdot \nabla b$ is over-loaded so that $(a, b) \cdot \nabla (c, d) \equiv (a \cdot \nabla c, b \cdot \nabla d)$. This part of the calculation is performed using Toro's Weighted Average Flux method (Ref. 12) which allows tight control to be maintained over any spurious diffusion of vorticity or particulate density from cell to cell as a result of numerical truncation errors.

Finally the vorticity distribution is corrected for the effects of stretching by advancing the solution to

$$\frac{\partial}{\partial t} \omega - \omega \cdot \nabla v = 0 \quad (27)$$

through Δt using Runge-Kutta integration, and initial conditions ω^{**} to obtain the solution ω^{***} . The vector $(\omega^{***}, \rho_s^{1**}, \dots, \rho_s^{N**})$ is then a second-order approximation to $\Omega(x, t + \Delta t)$ as long as Ω^* and Ω^{**} are both second-order accurate approximations to the solutions of their own differential equations (Ref. 5). The process is then repeated for subsequent timesteps. The similarity of this approach to that used by the fluid-only version of the VTM can be assessed by comparing this sequence of operations to that described in Ref. 5.

In the calculations presented in this paper, no non-equilibrium processes were accounted for, but these could be included in the calculation through an additional step that has similar form to that used to evolve the solution to Eq. 25.

Verification of Ground Effect Predictions

An important pre-requisite to the correct modeling of brownout is that the flow field generated by the rotorcraft in ground effect should itself be modeled accurately. This is no trivial requirement. A number of theoretical studies of ground effect, focusing particularly on thrust and power requirements at various rotor heights above the ground, have been published. Betz (Ref. 13) and Knight and Hefner (Ref. 14) for example showed that the power required to maintain a constant thrust reduces in ground effect and that the effect of the ground reduces significantly at heights above one rotor diameter. Cheeseman and Bennett (Ref. 15) reported on the effects of the ground during forward flight, showing that the power required to maintain a constant thrust increases with increasing forward

speed. Hayden (Ref. 16) provides a comprehensive review of power and thrust requirements for a range of helicopters hovering in ground effect that were obtained from flight test data and confirms that the greatest effect of the ground is felt at a height of less than one rotor diameter.

Most importantly in the present context, the experimental work of Sheridan and Wiesner (Ref. 17) and Curtiss et al. (Refs. 18, 19) has shown that the rotor wake exists in a number of distinct states, depending on the thrust-normalized advance ratio

$$\mu^* = \frac{\mu}{\sqrt{(C_T/2)}} \quad (28)$$

and height of the rotor above the ground. In hover, the wake is distorted significantly by the presence of the ground, and, indeed, at very low forward flight speed, the wake can be recirculated erratically through the front of the rotor. At intermediate forward speeds, the wake changes structure and a stable, bow-shaped ground vortex forms beneath the rotor. As the system is accelerated further, the ground vortex is swept downstream and the effect of the ground on the performance of the rotor reduces dramatically as the rotor accelerates over a narrow range of flight speeds. This characteristic behavior, and its dependence on aircraft geometry and flight condition, must be captured accurately in order for the dynamics of the sand cloud that is associated with the development of brownout to be modeled correctly.

The main impediment to accurate modeling of the flow that is induced by the rotor when in ground effect is that the dominant flow structures grow and evolve over very long time-scales. Simulations must thus resolve the wake accurately over many rotor revolutions in order to yield a valid portrayal of the governing fluid mechanics. As an example, Fig. 3 shows how approximately twenty five rotor revolutions have to elapse from the start of any simulation before the transients within the calculation dissipate, the system settles into its true long-term behavior, and the low-frequency unsteadiness in the power that is characteristic of the rotor dynamics when in ground effect is revealed. The VTM has been shown to be capable of conserving the wake structure almost indefinitely which gives the model an important advantage in being able to capture the slowly-evolving features of the flow that dominate the behavior of the system when in strong ground effect.

Figure 4 illustrates the ability of the VTM to capture the dependence of the structure of the wake on the forward speed of the rotor. The wake structure predicted by the VTM is visualized at various forward speeds by plotting snapshots of the vorticity distribution within the flow. Figure 4(a) shows the wake geometry at low advance ratio and reveals significant recirculation of the wake through the front of the rotor. At the slightly higher advance ratio shown in Fig. 4(b), a much more stable ground vortex forms below the rotor. As the advance ratio is increased further, the ground vortex moves backwards below the rotor

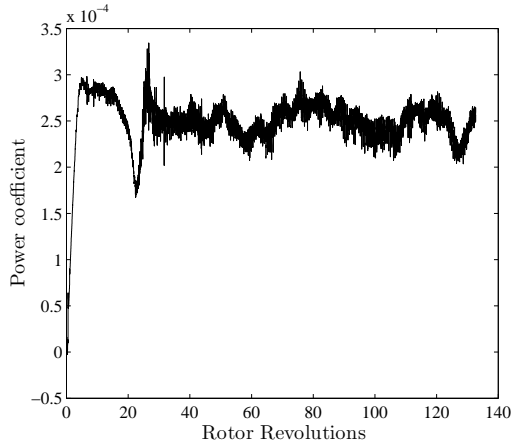


Figure 3: Example calculation showing the number of rotor revolutions that need to be simulated if rotor behavior IGE is to be captured accurately. Induced power required for a rotor hovering at $1.27R$ above the ground. ($C_T = 0.0046$).

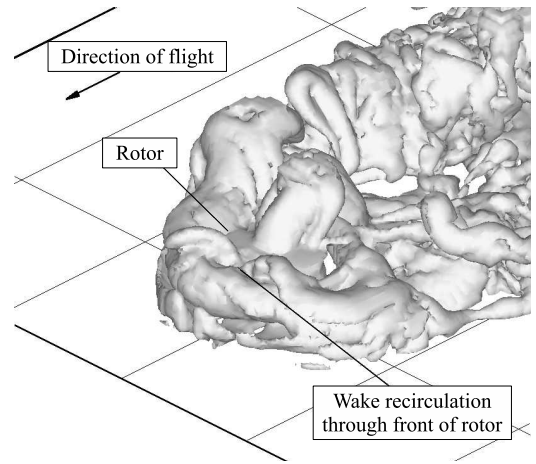
until it is eventually swept downstream to yield the wake geometry shown in Fig.4(c). The changes in computed wake geometry with forward speed are entirely consistent with the existence of the various flow regimes that were revealed in the experimental data of Curtiss et al. (Ref. 18).

As a more quantitative verification of the VTM, Fig. 5 shows a comparison between VTM predictions, various empirical correlations and the flight test data for the AH-1G collected by Hayden (Ref. 16) for the power required by a rotor to hover in ground effect at constant thrust. The VTM captures well the experimentally-observed decrease in the effect of the ground on the power required to hover as the height of the rotor above the ground is increased.

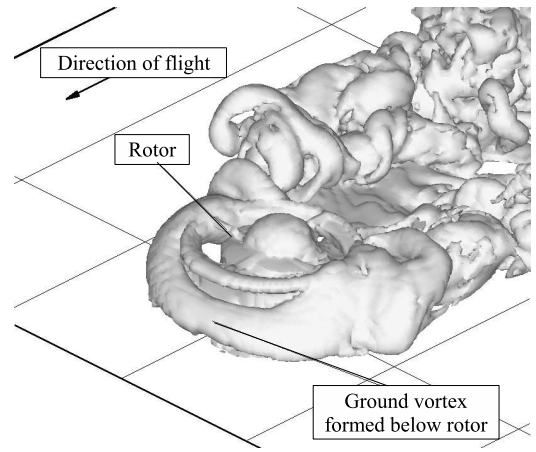
A detailed analysis of the changes in wake structure and the associated perturbations to rotor trim that are predicted by the VTM as a function of forward speed and height above the ground is presented by Brown and Whitehouse (Ref. 20). Taken together with the results presented in Figs. 4 and 5, these results illustrate the ability of the VTM to reproduce both the qualitative and quantitative aspects of the flow field that is generated by a rotor in strong ground effect.

Verification of Particulate Transport Predictions

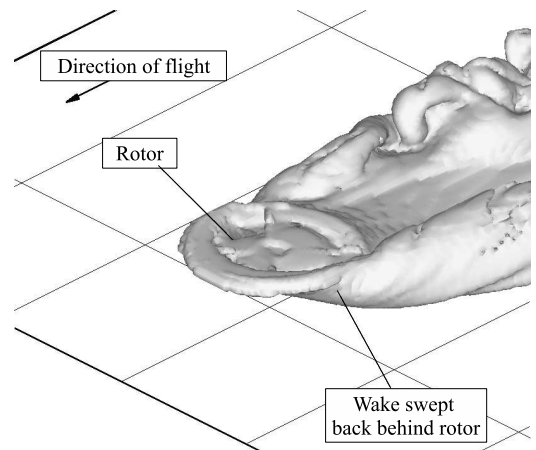
To date, very limited experimental data is available that can be used directly to verify the predictions of numerical brownout models. A recent experimental study carried out at the University of Glasgow (Ref. 22) has allowed some confidence to be placed in the predictions of the VTM, however. The experiment involved placing fine particles on the floor of a wind tunnel below a small model rotor to



(a) Recirculation regime ($\mu^* = 0.61$).



(b) Ground vortex regime ($\mu^* = 0.8$).



(c) High-speed regime ($\mu^* = 1.3$).

Figure 4: Rotor wake geometry at various forward speeds (rotor at height of $0.68R$ above ground).

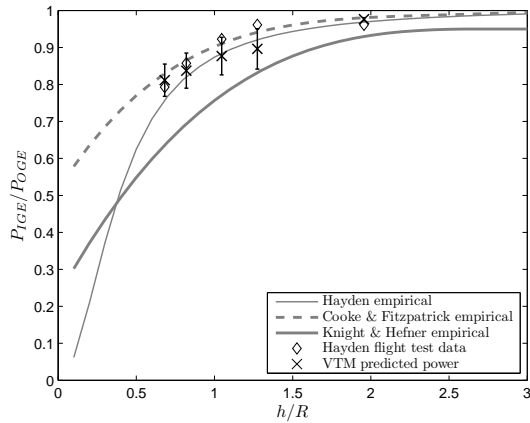


Figure 5: Power required to hover IGE. VTM predictions compared to the flight test data and empirical correlations of Hayden (Ref. 16), Knight & Hefner (Ref. 14) and Cooke & Fitzpatrick (Ref. 21) for a rotor operating at various heights above the ground ($C_T = 0.0046$). Bars attached to the VTM data represent the predicted root-mean-square of the power fluctuations produced by the rotor.

simulate the dynamics of the dust particles that would be entrained into the flow around the rotor in a brownout situation. The motion of the particles as they were transported through the flow surrounding the rotor was recorded using high-speed photography. Figures 6(a) and (b) show typical snapshots of the particle distribution in front of the model rotor when it was placed at one radius above the ground and the tunnel speed was set to represent a thrust-normalized advance ratio of 0.65. For comparison, Fig. 7 shows a representative snapshot of the particle density distribution in front of the rotor that is predicted by the VTM under similar flight conditions. The experiment reveals a wedge-shaped area in the flow some distance upstream of the rotor, termed the ‘separation zone’ by Nathan and Green (Ref. 22), in which the particle density is very high as a result of the existence of a flow stagnation line in the mean flow on the surface below. Figure 7 shows the location and size of this zone to be represented well by the VTM. Figure 6(a) shows a significant proportion of the suspended particulate matter to be recirculated through the front of the rotor disk under the operating conditions of the experiment, but Fig. 6(b), captured at a later time during the same experiment, shows that clouds of particles that do not recirculate through the rotor are also ejected sporadically from the separation zone. Figure 7 shows both these characteristic features of the dynamics of the dust cloud surrounding the rotor to be captured by the VTM.

Although a more quantitative verification of the numerical approach awaits further refinement of the experimental technique, the good qualitative agreement between the particulate density distributions that are predicted by the VTM

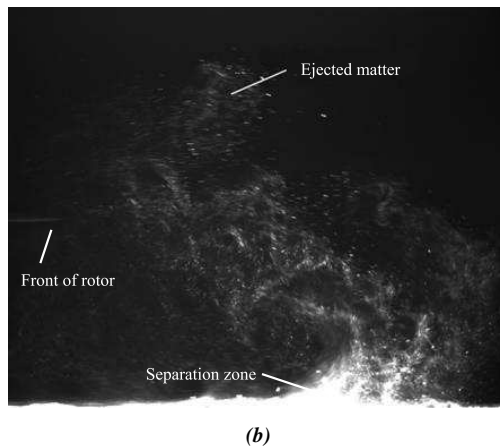
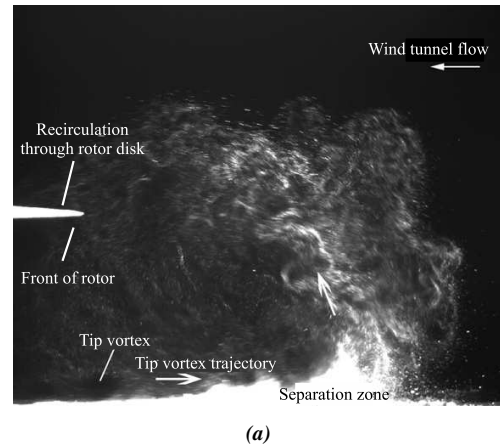


Figure 6: Snapshots of the particulate distribution around a rotor during wind tunnel simulations of brownout. Blade tip visible at middle left. (a) Image showing the recirculation of fine particulates through the front of the disk and the existence of a well-defined ‘separation zone’ above the ground plane. (b) Image showing the escape of a cloud of particles from the main recirculatory flow. Images courtesy of Richard Green, University of Glasgow.

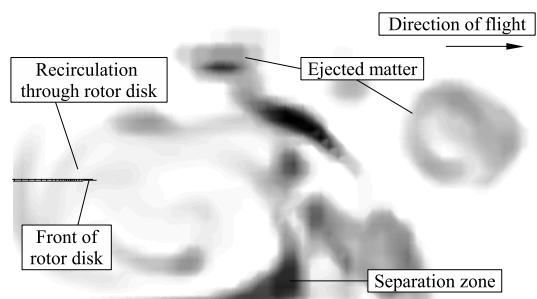


Figure 7: VTM-predicted particulate density distribution on a vertical slice through the rotor centerline under the same flight conditions as Fig. 6, showing qualitatively the same features as the experiment.

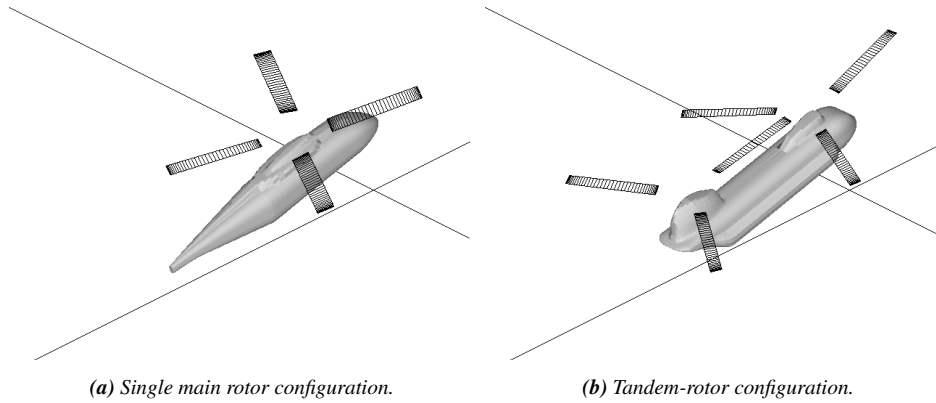


Figure 8: Simulated helicopter geometries.



(a) Tandem-rotor configuration.



(b) Single main rotor configuration.

Figure 9: Dust distribution in the airflow surrounding a helicopter operating at low altitude in desert conditions. Images courtesy of U.S. Department of Defense.

and the distribution of particulates that were observed in this simple experiment suggests that the VTM is capable of producing credible simulations of the evolution of the dust cloud surrounding the helicopter under brownout conditions.

Simulation of Brownout Development

As an initial test of the capabilities of the approach, the coupled VTM-particulate transport model has been used to

compare the geometry and extent of the dust cloud that is generated under brownout conditions by the two generic helicopters shown in Fig. 8. Anecdotal evidence suggests that, under practical conditions, brownout manifests rather differently for helicopters with a single main rotor, such as that shown at left in the figure, than for aircraft with the tandem-rotor configuration shown at right. In particular, the dust cloud generated by the rear rotor of the tandem configuration is thought to run forward during landing to eventually engulf the cockpit, whereas the dust cloud of the single rotor system is thought to originate somewhat further forward, upstream of the ground vortex, and to engulf the helicopter in more sudden fashion as the helicopter nears the ground. These observations are partially confirmed by images, such as those shown in Fig. 9, of the dust clouds that are generated by the two different types of helicopter when flown at low level in dusty conditions. Although there are indeed likely to be very strong qualitative differences between the way that brownout conditions manifest for the two different rotor configurations, it should be borne in mind that simplistic descriptions and gross generalizations such as the one just given soon prove inadequate once the operating conditions and detailed geometry of the helicopter are considered in more detail. The geometry and extent of the helicopter-generated dust cloud appears to be strongly dependent, for instance, on how the aircraft is maneuvered over the ground as the dust cloud begins to form.

Some care was taken to define the two simulated helicopters to provide a fair comparison between the behavior of single main rotor and tandem-rotor configurations. Both simulated helicopters were defined with the same rotor diameter and overall blade area, and in both cases were trimmed to an overall thrust coefficient of 0.0145. The systems thus have ostensibly the same blade loading, and should thus produce wakes of very similar strength. The resultant dust density distributions in the flow surrounding the two configurations can thus be compared directly if the two helicopters are flown at the same thrust-normalized ad-

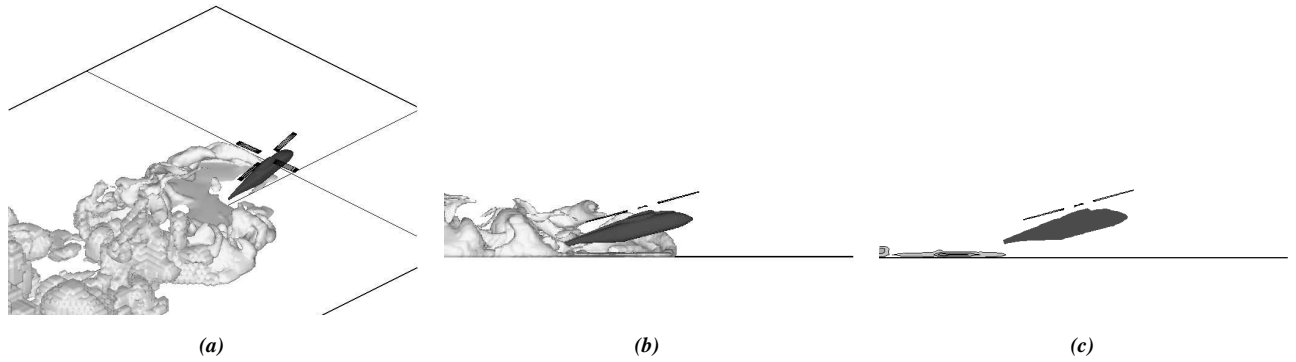


Figure 10: VTM-predicted dust distribution surrounding a helicopter with single main rotor configuration ($\mu^* = 0.80$).

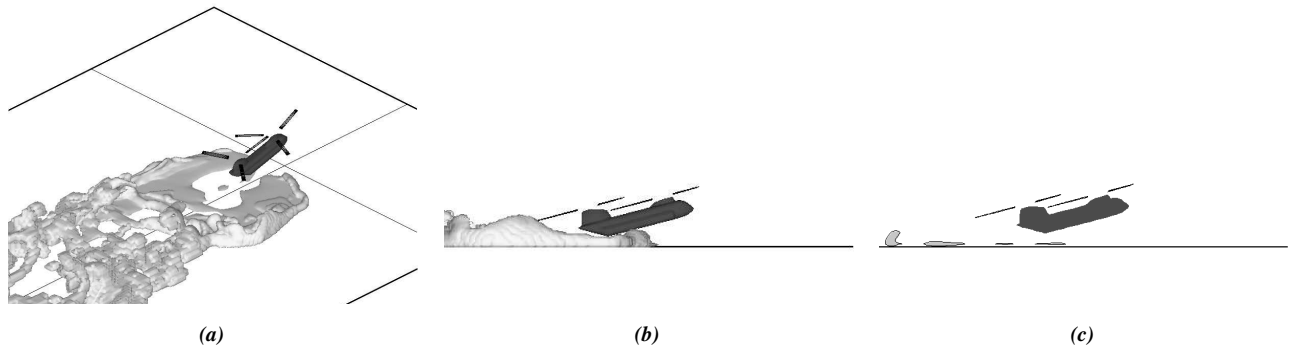


Figure 11: VTM-predicted dust distribution surrounding a helicopter with tandem-rotor configuration ($\mu^* = 0.80$).

vance ratio. In all cases the wake was resolved using 40 computational cells across the rotor diameter.

The helicopters were modeled with a nose-up pitch attitude of 15° to represent the aircraft during the late stages of a landing maneuver. Somewhat unrealistically, this pitch attitude and also the rotor height above the ground was maintained throughout the maneuver. Given that the trajectory of the aircraft is thought to have such a strong influence on the formation of the dust cloud, future efforts will be focused on extending the model to allow the dynamics of the vehicle above the ground to be represented in a more comprehensive fashion.

Figures 10 through 17 show the geometry of the dust cloud that is predicted by the VTM with the helicopters at various forward flight speeds during the simulated deceleration to land. A three-dimensional view of the dust cloud is shown at left in each of these figures by plotting an iso-surface of dust density within the flow surrounding the helicopter. At center, the same iso-surface is represented, but from a side perspective so that the vertical extent of the dust cloud relative to the operating height of the helicopter can be appreciated. At right, contours of dust density on a vertical slice through the flow around the helicopter, on a plane that coincides with the centerline of the fuselage, are shown. These contour plots show the dust density in

the flow around the helicopter, averaged over 60 rotor revolutions to yield an appreciation of the most persistent features in the dust cloud. The minimum contour level represented in the contour plots has the same value as the iso-surface value used to generate the 3-D plots. It is important to avoid contamination of the data by vortical or particulate structures that arise simply in the initial conditions that were applied to the simulations and for this reason the figures present the dust distributions in the flow around the helicopters at a time far enough into the simulations for the flow to have settled into its long-term behavior.

Figures 10 and 11 show the dust cloud that is created by the two configurations when flying at a relatively high forward speed above the ground. At the advance ratio $\mu^* = 0.80$ of these figures, the wakes of both configurations operate in the ground vortex state, although at this forward speed the ground vortex is relatively compact and forms some distance behind the leading edge of the rotors. The major interaction between the wake and the ground thus occurs some distance behind the nose of the helicopter in both cases. As a result, at this advance ratio the aircraft remains in the clear air ahead of the majority of the dust that is entrained from the ground into the flow. A low, crescent-shaped ridge of dust marks the advancing front of the dust cloud below the aircraft – this ridge forms on the

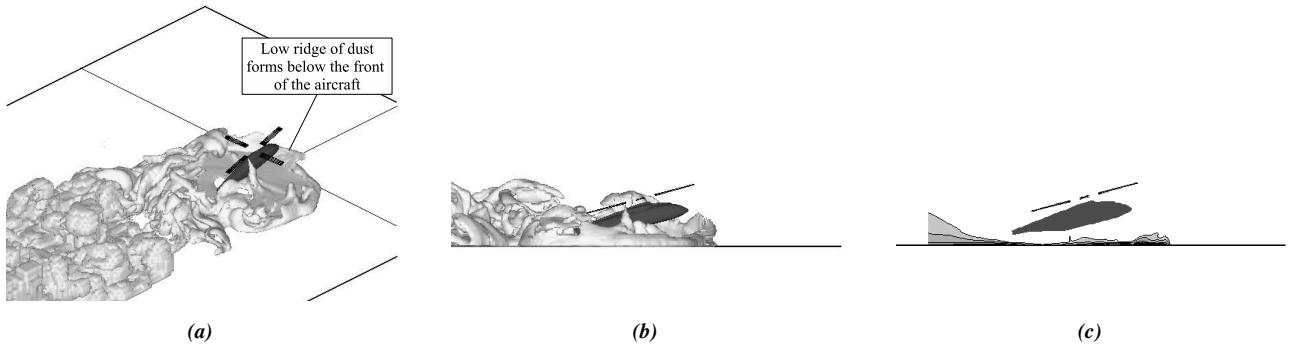


Figure 12: VTM-predicted dust distribution surrounding a helicopter with single main rotor configuration ($\mu^* = 0.47$).

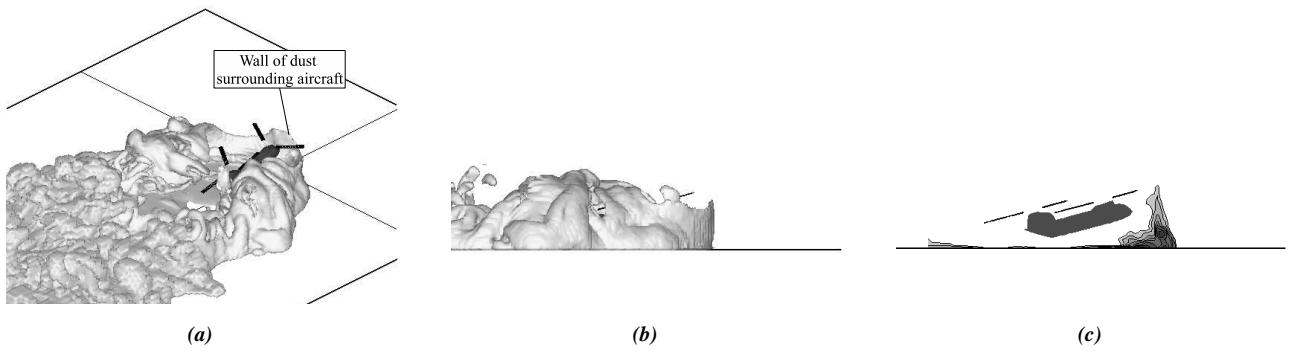


Figure 13: VTM-predicted dust distribution surrounding a helicopter with tandem-rotor configuration ($\mu^* = 0.47$).

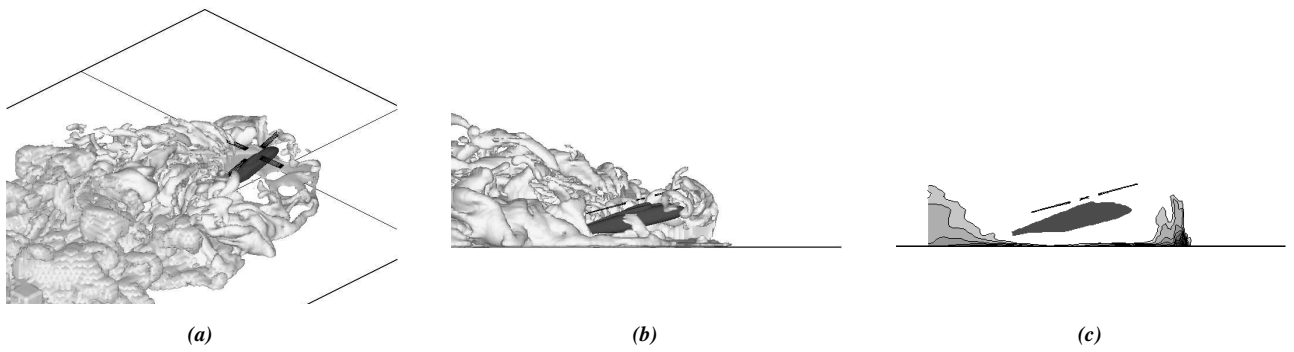


Figure 14: VTM-predicted dust distribution surrounding a helicopter with single main rotor configuration ($\mu^* = 0.29$).

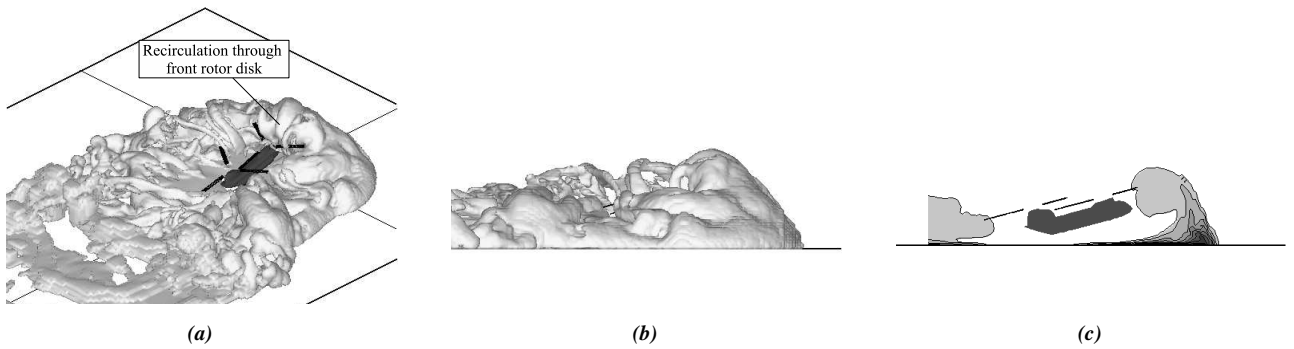


Figure 15: VTM-predicted dust distribution surrounding a helicopter with tandem-rotor configuration ($\mu^* = 0.29$).

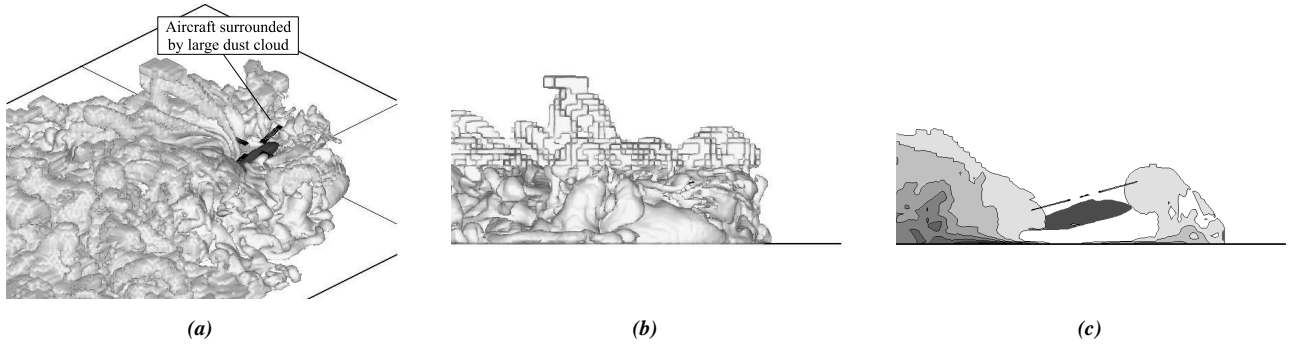


Figure 16: VTM-predicted dust distribution surrounding a helicopter with single main rotor configuration ($\mu^* = 0.12$).

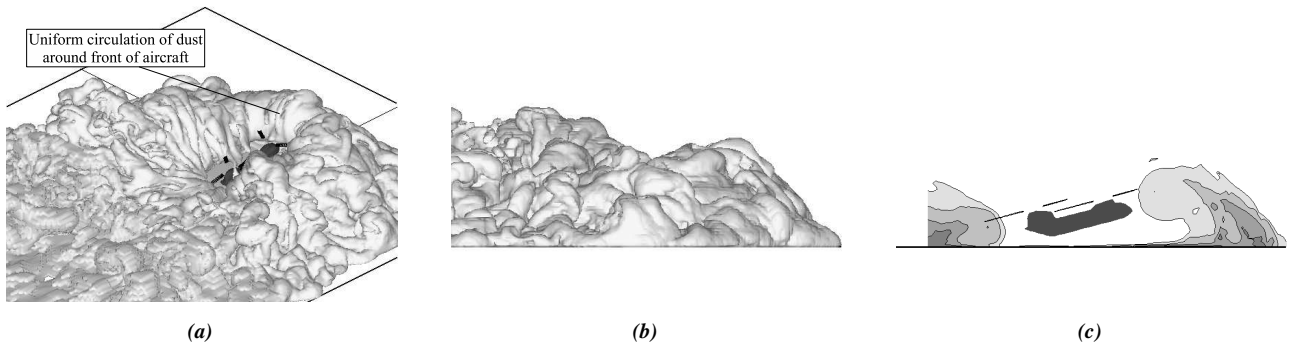


Figure 17: VTM-predicted dust distribution surrounding a helicopter with tandem-rotor configuration ($\mu^* = 0.12$).

ground some distance behind the nose of the aircraft and extends outwards and downstream, following the location of the separation zone that forms along the forward edge of the ground vortex that is generated by the helicopter. The interaction between the wakes of the front and rear rotors of the tandem configuration appears to yield a more rearwards location of the ground vortex and associated dust cloud than the single main rotor configuration under the same flight conditions.

The iso-surface plots of dust density show the single main rotor configuration to generate a distinctly asymmetrical dust cloud (with a marked absence of dust to the right of the aircraft – the rotor of this helicopter was arranged to rotate anticlockwise when viewed from above). In comparison, the tandem-rotor configuration generates a dust cloud that spreads out symmetrically on both sides of the aircraft at this forward flight speed. Unfortunately the asymmetry of the dust cloud generated by the helicopter with single main rotor does not seem to persist to the very lowest forward flight speeds where it might be exploited practically to mitigate the effects of brownout.

To explain the asymmetry in the dust cloud, Fig. 18 compares the vorticity distribution to the corresponding dust distribution in the flow around the helicopter with single main rotor. For comparison, Fig. 19 shows similar plots for the tandem-rotor configuration. The iso-surface used to

represent the vorticity distribution has been chosen to reveal the strongest vorticity that is present in the flow. The powerful, crescent-shaped ground vortex that lies below each helicopter is clearly shown, but the plot also reveals that, for the helicopter with a single main rotor, this structure is significantly asymmetric. The core of the ground vortex remains significantly closer to the ground on the left-hand side of the aircraft than on the right as the helicopter moves forwards along the ground. The tandem-rotor helicopter, on the other hand, generates a ground vortex that has a far more symmetric structure. Any asymmetry in the dust cloud is then explained by the clear correlation between the region of maximum entrainment of dust into the air and the position and strength of the ground vortex that is evident on comparing parts (a), (b) and (c) of the figures.

Figures 12 and 13 show the dust cloud that the VTM predicts to form around the helicopters once they have decelerated to an advance ratio $\mu^* = 0.47$. At this forward speed, the wake of an isolated, horizontal rotor would exist within the recirculation regime, but the rearwards tilt of the rotors under the simulated conditions causes instead a fairly large and coherent ground vortex to form just forward of the helicopters. Most interestingly, the iso-surface plots of the dust density distribution around the single main rotor configuration show a fairly broad region surrounding the helicopter in which the dust layer remains sheet-like

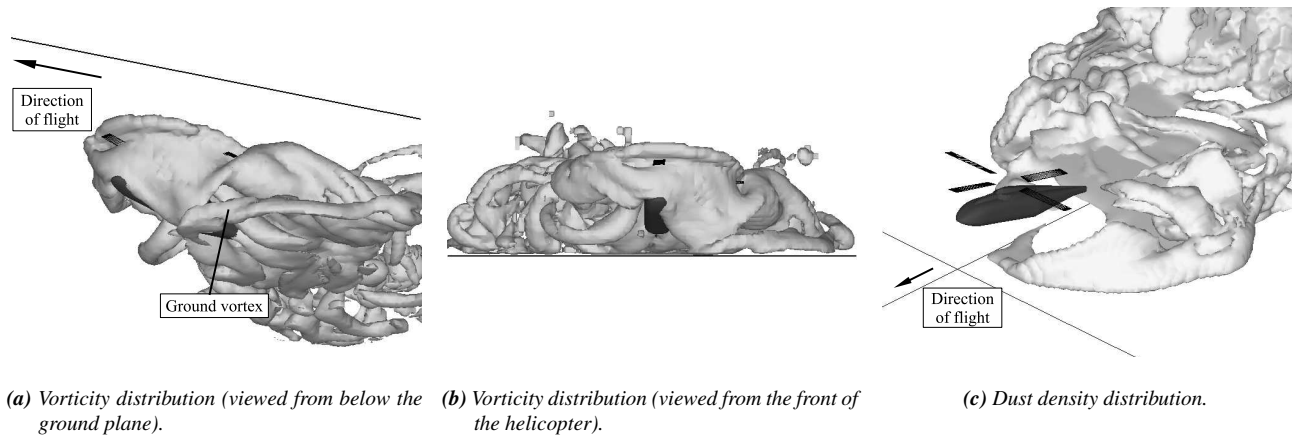


Figure 18: Correlation between the vorticity distribution surrounding a helicopter with single main rotor and the regions of maximum entrainment of dust into the flow. ($\mu^* = 0.80$).

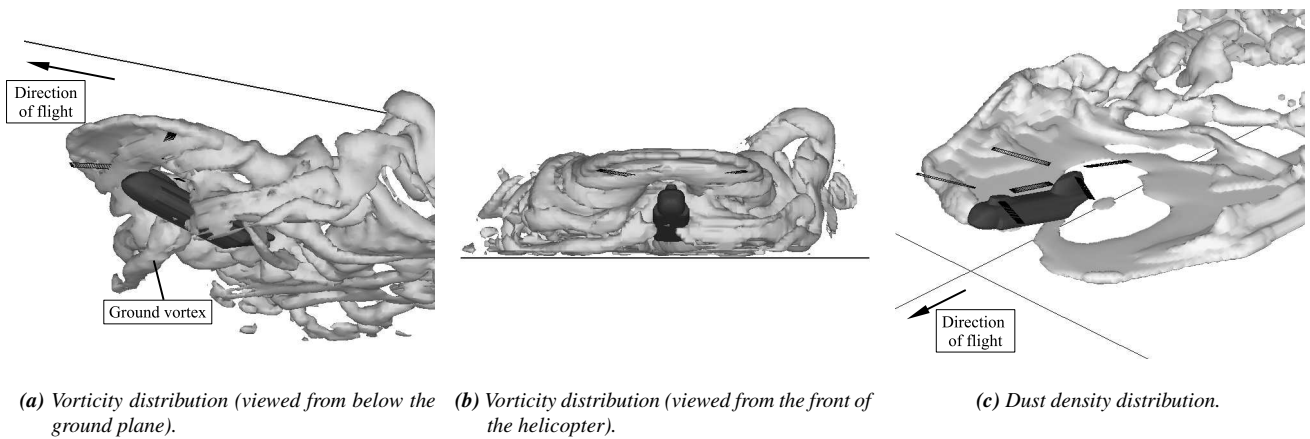


Figure 19: Correlation between the vorticity distribution surrounding a tandem-rotor helicopter and the regions of maximum entrainment of dust into the flow. ($\mu^* = 0.80$).

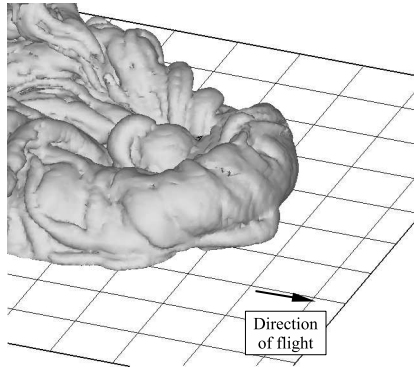
and very close to the ground. Even where the dust is lifted into the flow, the resultant cloud remains relatively close to the ground. In contrast, the dust cloud forms very much closer to the tandem-rotor configuration and has significant vertical extent. Indeed, the plots of the averaged dust density on the longitudinal slice through the flow show the wall of dust that forms in front of the aircraft with single main rotor to be diffuse and somewhat tenuous in comparison to the thick, persistent wall of dust that forms directly in front of the tandem-rotor aircraft at this forward speed.

Further deceleration of the helicopters results in a significant enlargement of the dust cloud that surrounds the aircraft, particularly as the wake transitions from the ground vortex regime into the recirculatory regime. Figures 14 and 15 show the dust distribution in the flow with the aircraft travelling above the ground at advance ratio $\mu^* = 0.29$. At this advance ratio the rotors operate well within the recirculatory flow regime. Nevertheless, a comparison of the averaged dust density on the longitudinal slice through the

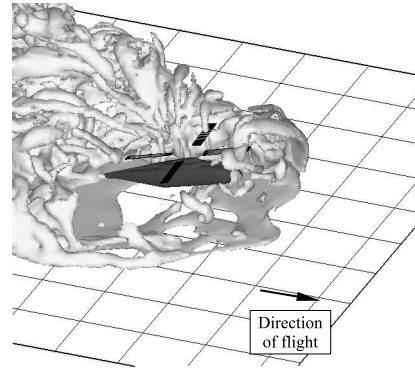
flow shows the tandem-rotor configuration to continue to produce a dust cloud that is far larger and more persistent, and that extends significantly higher above the helicopter, than the cloud that is produced by the single main rotor configuration.

In similar vein to Figs. 18 and 19, Figs. 20 and 21 contrast the vorticity and dust density distributions in the flow around the two helicopter configurations at this low forward speed. The much enlarged region of strong vorticity that forms in front of the helicopter with the rotors operating in the recirculatory regime is principally responsible for transporting dust high into the air surrounding the helicopter from its origin on the ground plane. The key role of the separation zone just forward of the recirculatory flow in limiting the forward extent of entrainment of dust from the ground, and hence in governing the overall size of the dust cloud, is clearly evident on comparing the vorticity and dust distributions within the flow.

Further deceleration of the aircraft results in both config-

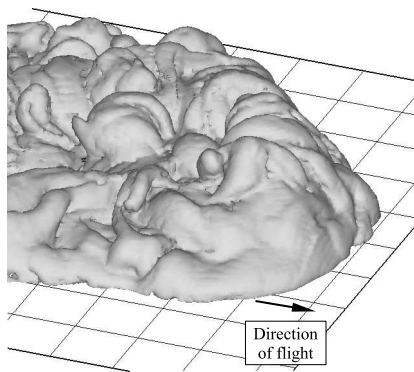


(a) Vorticity distribution.

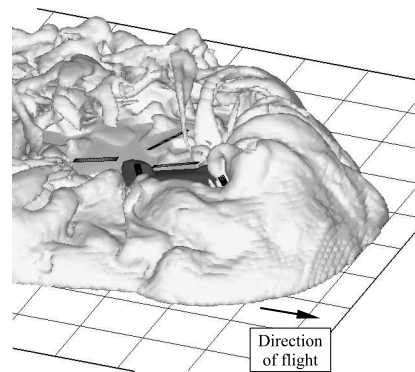


(b) Dust density distribution.

Figure 20: Correlation between the vorticity distribution surrounding a helicopter with single main rotor and the regions of maximum entrainment of dust into the flow. ($\mu^* = 0.29$).



(a) Vorticity distribution.



(b) Dust density distribution.

Figure 21: Correlation between the vorticity distribution surrounding a tandem-rotor helicopter and the regions of maximum entrainment of dust into the flow. ($\mu^* = 0.29$).

urations becoming engulfed in a large and persistent cloud of dust. Figures 16 and 17 show the predicted dust cloud around the aircraft when flying above the ground at very low forward speed ($\mu^* = 0.1174$). Significant recirculation of dust through the rotor disks is clearly evident in both cases, and it is quite plausible that in practical circumstances the density and persistence of the dust cloud might precipitate the onset of brownout conditions.

The results presented here thus reveal distinct differences in the geometry of the dust cloud that is formed by single main rotor and tandem-rotor configurations when operating at low altitude and forward speed above a dusty surface, and it appears that at least some of these differences can be related to the geometry of the vorticity distribution that is produced by the rotors as they interact aerodynamically with the ground surface.

Conclusion

This paper presents a computational model for simulating the development of the dust cloud that is associated with the

particulate matter that can be entrained into the air when a helicopter is operated close to the ground in desert or dusty conditions. The physics of this problem, and the associated pathological condition known as ‘brownout’ where the pilot loses situational awareness as a result of his vision being occluded by dust suspended in the flow around the helicopter, is acknowledged to be very complex, and, indeed, modeling of the brownout problem from first principles poses many basic challenges.

The approach advocated here involves an approximation to the full dynamics of the coupled particulate-air system. Away from the ground, the model that is derived in this paper relies on the simplifying assumption that the suspended particulate matter remains in near equilibrium under the action of the aerodynamic forces that are generated by the particles as they move relative to the air. Close to the ground where this assumption begins to fail, this representation of the dynamics of the particulates is replaced with a sublayer type source model in which the saltation process that is fundamental to the entrainment of particulates into

the air is modeled algebraically. As the state of the art advances, it may indeed be possible to supplant this approach using a model that is based on a more fundamental physical description, but certainly the extreme complexity of the physics within the dense layer of strongly interacting particles close to the ground precludes this approach for the time being.

The advantage of the present approach is that the growth in the number of free parameters within the model is strongly curtailed – in fact, almost all of the tunable coefficients within the present implementation of the approach reside within the sublayer model itself. This should have distinct advantages for the reliability and robustness of the approach, and in many ways it can be argued that the model presented here may provide a more sensible, balanced and well-justified engineering approach to the analysis and eventual understanding of the brownout problem than some descriptions of the problem that embody a more complete set of physical processes and effects.

Most computational codes are written in an Eulerian frame of reference, whereas the most obvious description of the dynamics of individual particles is in a Lagrangian frame of reference. Using the basic principles of statistical mechanics, the Lagrangian and Eulerian descriptions of the problem can be reconciled, however. The advantage of such an analysis is that it provides an inherent method of quantifying its own assumptions – indeed, it has been shown how the validity of the method can be evaluated in context by comparing the spectrum of physical properties of the suspended particulates to the local properties of the flow field surrounding the helicopter.

The result is a particulate transport model that resides in the Eulerian frame of reference and that, because of its particular mathematical form, can be integrated in fairly straightforward manner into other models that describe the dynamics of the fluid in terms of the Eulerian transport of the fluid properties. The VTM helicopter simulation code is used here to host the particulate transport model, and, indeed, possesses particular advantages with respect to the computational implementation of the coupled fluid-particle model because of the very close similarities in structure between the particulate transport equation and the vorticity transport equation.

Verification of the predictions of the method remains problematic at this early stage in investigations into the brownout phenomenon, however. A significant quantity of data resides within the environmental fluid dynamics community, but it is not immediately obvious how relevant this data is given the rather different length and time-scales that are important within the flow field that is induced by a helicopter flying close to the ground. This presents some concerns as to whether the choice of sublayer model used in the present study, based as it is on work conducted in the field of aeolian and riverine sediment transport, is entirely appropriate in the context of brownout modeling. Full veri-

fication of the approach awaits further developments in experimental technique and the gathering of data that is directly relevant to the brownout problem, but limited comparisons against small-scale rotor experiments show encouraging results.

An important pre-requisite of any model of brownout is the ability to capture the basic characteristics of the flow that is induced by the helicopter rotors when in strong ground effect; the VTM has been demonstrated to perform well in this respect. Particularly important in the present context appears to be the ability of the model to predict the transition of the wake generated by the helicopter between several characteristic states as the speed of the helicopter above the ground is varied. This is by no means a trivial task as it requires careful preservation of the vortical structures in the wake for the many rotor revolutions that characterize the timescales over which the rotor-induced flow evolves in the presence of the ground.

An example application of the coupled VTM-particulate transport model to analyzing the differences in the geometry and extent of the dust clouds that are produced by single main rotor and tandem-rotor configurations as they decelerate to land has yielded some very interesting results. Although the simulations described here are based on a rather simplified representation of the helicopter landing maneuver, it appears, somewhat surprisingly, that relatively coarse features of the geometry and strength of the rotor wakes, in particular the location of the ground vortex and the size of any regions of recirculatory flow, should they exist, play a primary role in governing the extent of the dust cloud that is created by the helicopter.

Much work still remains to be done in conducting and dissecting simulations such as these to elucidate the key parameters that govern the evolution of the dust cloud that is generated by the aerodynamic interaction between the helicopters and the ground when these machines operate at low level in dusty environments. The results presented here represent perhaps a small step along the way to a sufficient practical understanding of how the physics of particle entrainment and transport within the flow around the helicopter can precipitate the onset of brownout conditions, but hopefully they also provide some encouragement that the problem may eventually yield to careful engineering analysis.

References

- ¹ Keller, J.D., Whitehouse, G.R., Wachspress, D.A., Teske, M.E., and Quackenbush, T.R., "A Physics-Based Model of Rotorcraft Brownout for Flight Simulation Applications," 62nd Annual Forum of the American Helicopter Society, Phoenix, AZ, May 2006.
- ² Crowe, C.T., Ed., *Multiphase Flow Handbook*, CRC Press, Boca Raton, FL, 2006.
- ³ Leishman, J.G., *The Helicopter - Thinking Forward*,

- Looking Back*, College Park Press, College Park, MD, 2007.
- ⁴ Ryerson, C.C., Hachnel, R.B., Koenig, G.G., and Moulton, M.A., "Visibility Enhancement in Rotorwash Clouds," 43rd AIAA Aerospace Sciences Meeting and Exhibit, Reno, Nevada, Jan 2005.
 - ⁵ Brown, R.E., "Rotor Wake Modeling for Flight Dynamic Simulation of Helicopters," *AIAA Journal*, Vol. 38 (1), January 2000, pp. 57–63.
 - ⁶ Brown, R.E. and Line, A.J., "Efficient High-Resolution Wake Modeling Using the Vorticity Transport Equation," *AIAA Journal*, Vol. 43 (7), July 2005, pp. 1434–1443.
 - ⁷ Marticorena, B. and Bergametti, G., "Modeling the Atmospheric Dust Cycle: 1. Design of a soil-derived dust emission scheme," *Journal of Geophysical Research*, Vol. 100 (D8), August 1995, pp. 16415–16430.
 - ⁸ Lu, H. and Shao, Y., "Toward Quantitative Prediction of Dust Storms: An Integrated Wind Erosion Modelling System and its Applications," *Environmental Modelling and Software*, Vol. 16 (3), April 2001, pp. 233–249.
 - ⁹ MacKinnon, D.J., Clow, G.D., Tigges, R.K., Reynolds, R.L., and Chavez, P.S. Jr., "Comparison of Aerodynamically and Model-derived Roughness Lengths (Z_0) Over Diverse Surfaces, Central Mojave Desert, California, USA," *Geomorphology*, Vol. 63 (1–2), November 2004, pp. 103–113.
 - ¹⁰ White, B.R., "Soil Transport by Winds on Mars," *Journal of Geophysical Research*, Vol. 84 (B9), August 1979, pp. 4643–4651.
 - ¹¹ Cheng, N.-S., "Simplified Settling Velocity Formula for Sediment Particle," *Journal of Hydraulic Engineering*, Vol. 123 (2), February 1997, pp. 149–152.
 - ¹² Toro, E.F., "A Weighted Average Flux Method for Hyperbolic Conservation Laws," *Proceedings of the Royal Society of London, Series A: Mathematical and Physical Sciences*, Vol. 423 (1864), 1989, pp. 401–418.
 - ¹³ Betz, A., "The ground Effect on Lifting Propellers," Tech. Rep. NACA TM 836, August 1937.
 - ¹⁴ Knight, M. and Hefner, R.A., "Analysis of Ground Effect on the Lifting Airscrew," Tech. Rep. NACA TN 835, 1941.
 - ¹⁵ Cheeseman, I.C. and Bennett, W.E., "The Effect of the Ground on a Helicopter Rotor in Forward Flight," Tech. Rep. ARC R & M 3021, Aeronautical Research Council, 1957.
 - ¹⁶ Hayden, J.S., "The Effect of the Ground on Helicopter Hovering Power Required," 32nd Annual Forum of the American Helicopter Society, Washington, D.C., May 1976.
 - ¹⁷ Sheridan, P.F. and Wiesner, W., "Aerodynamics of Helicopter Flight Near the Ground," 33rd Annual Forum of the American Helicopter Society, Washington DC, May 1977.
 - ¹⁸ Curtiss, H.C. Jr., Erdman, W., and Sun, M., "Ground Effect Aerodynamics," *Vertica*, Vol. 11 (1–2), 1987, pp. 29–42.
 - ¹⁹ Curtiss, H.C. Jr., Sun, M., Putman, W.F., and Hanker, E.J. Jr., "Rotor Aerodynamics in Ground Effect At Low Advance Ratios," *Journal of the American Helicopter Society*, Vol. 29 (1), 1984, pp. 48–55.
 - ²⁰ Brown, R.E. and Whitehouse, G.R., "Modelling Rotor Wakes in Ground Effect," *Journal of the American Helicopter Society*, Vol. 49 (3), July 2004, pp. 238–249.
 - ²¹ Cooke, A.K. and Fitzpatrick, E.W.H., *Helicopter Test and Evaluation*, American Institute of Aeronautics and Astronautics Education Series, Reston, VA, 2002.
 - ²² Nathan, N.D. and Green, R.B., "Measurements of a Rotor Flow in Ground Effect and Visualisation of the Brown-out Phenomenon," 64th Annual Forum of the American Helicopter Society, Montréal, Canada, 2008.